DOI: 10.1002/cbic.200500172

Design, Synthesis and Analysis of Inhibitors of Bacterial Aspartate Semialdehyde Dehydrogenase

Russell J. Cox,*[a] Jennifer S. Gibson,[a] and Andrea T. Hadfield[b]

Unsaturated and fluorinated analogues of aspartyl-β-phosphate were synthesised as potential inhibitors of the bacterial enzyme aspartate semialdehyde dehydrogenase (ASA-DH). Acetylenic and Z-olefinic analogues showed competitive inhibition, but an E-olefinic analogue was inactive. A monofluoromethylene phosphonate competed poorly, but showed time-dependent inhibition of ASA-DH in the absence of phosphate. Simulated docking procedures were used to rationalise the results. These studies showed that substrate and inhibitor binding are mediated by interaction with two active-site arginine residues, and for likely covalent attachment to the active-site thiol group, electrophilic carbon atoms should be located 4.5 Å, or less, from the thiol.

Aspartate semialdehyde dehydrogenase (ASA-DH) is an enzyme that catalyses one of the first steps during the biosynthesis of cell-wall components and amino acids in bacteria (Scheme 1).[1] The enzyme catalyses the reductive dephosphorylation of aspartyl phosphate **1** using an active-site cysteine. The cysteine thiol attacks the acyl carbonyl of **1**, displacing phosphate and creating a thiolester **2**, which is covalently bound to the enzyme. The thiolester is then reduced by hydride from NADPH, releasing the active-site thiol and aspartate semialdehyde **3** from the active site.[2] Inhibition of ASA-DH would be expected to lead to cell lysis, and experiments in which the ASA-DH gene, *asd*, has been knocked out yield bacteria incapable of surviving in the absence of exogenous cell-wall precursors.[3] For this reason, potent inhibitors of ASA-DH could form a new class of antibacterial agents. We have previously reported the synthesis and properties of ASA-DH inhibitors based on the structure of the substrate, aspartyl phosphate **1**.[4] We now report the design, synthesis and testing of compounds designed to act as covalent inactivators of ASA-DH.

In previous work, we described the synthesis of analogues of **1**, in which the phosphate ester oxygen atom was replaced by CF_2, CH_2 or NH (compounds **4**–**6**, respectively).[4] These compounds were designed to mimic the substrate **1** but be incapable of losing phosphate. These compounds also allowed us to learn about substrate recognition in the active site of ASA-DH. The phosphate pK_{a_2} should be around 7 or higher for opti-

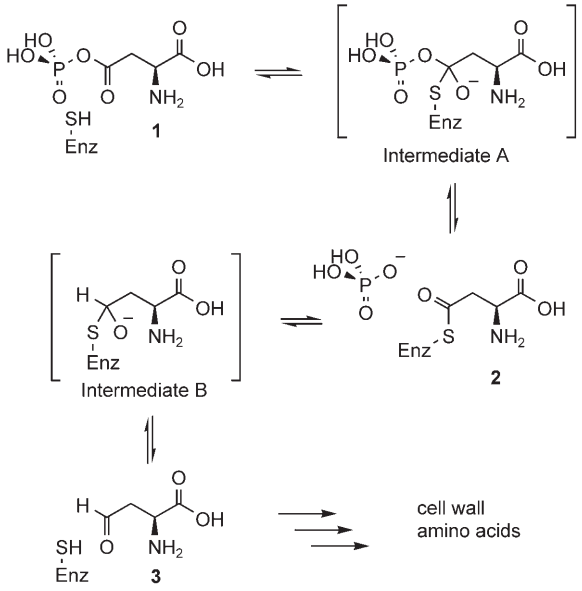

Scheme 1. Reactions catalysed by ASA-DH and biological fate of aspartate semialdehyde.

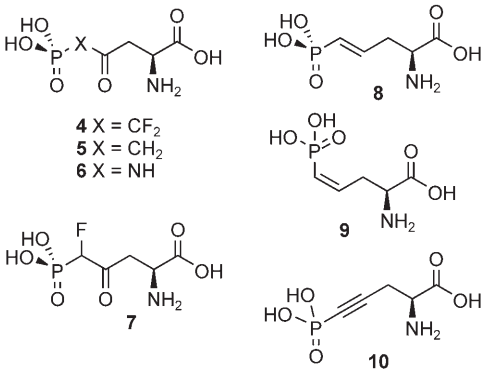

[a] *Dr. R. J. Cox, J. S. Gibson*
School of Chemistry, University of Bristol
Cantock's Close, Clifton, Bristol, BS8 1TS (UK)
Fax: (+44) 117-929-8611
E-mail: r.j.cox@bris.ac.uk

[b] *Dr. A. T. Hadfield*
Department of Biochemistry, School of Medical Sciences
University Walk, Clifton, Bristol, BS8 1TD (UK)

Supporting information for this article is available on the WWW under http://www.chembiochem.org or from the author.

mal binding,[4] so that the phosphate is mono-ionised at physiological pH. For the difluorophosphonate **4** with a pK_{a_2} of about 4.5, initial binding was therefore poor, while the phosphonate **5** ($pK_{a_2} \approx 6.1$) and phosphoramidate **6** ($pK_{a_2} \approx 6.3$) bound progressively better. However, another feature was also important—the high electrophilicity of the difluoromethylene carbonyl of **4** means that it most likely forms a reversible covalent bond with the active-site thiol of ASA-DH, leading to more potent slow-binding inhibition.[4] The design of compounds likely to be electrophilic at this carbon atom, while maintaining a relatively high pK_{a_2} value for the phosphorous moiety, was therefore considered.

Thus we considered compounds such as the monofluorophosphonate **7**, which would be expected to have a phosphonate pK_{a_2} value around 6.2[5] and a moderately electrophilic carbonyl group. The isomeric olefins **8** and **9**, expected to have pK_{a_2} values around 7.9[6] and likely Michael acceptors at the desired carbon atom were also considered. Finally, the acetylene **10** was chosen—analogous acetylenic esters are excellent Michael acceptors for thiols, and we expected the pK_{a_2} of the phosphonate to be around 6.3.[6] The more rigid unsaturated compounds would also allow us to assess possible steric requirements in the active site of ASA-DH.

Synthesis

Monofluorophosphonates have been reported before to be useful mimics of phosphates. For example, Berkowitz described fluorophosphonate analogues of glucose-6-phosphate (G6P) as alternative substrates for G6P-dehydrogenase[5] and O'Hagan has described fluorinated analogues of glycerol-3-phosphate as alternative substrates for glycerol-3-phosphate dehydrogenase.[7] In both cases the monofluorophosphonate proved to be a better substrate than methylene or difluoromethylene analogues.

We initially approached the synthesis of **7** using chemistry developed by Savignac—the generation of a lithiosilylfluoromethyl phosphonate **12** and its reaction with an activated carbonyl species (Scheme 2).[8] However, these reactions proved unproductive, and the desired protected monofluoromethylene phosphonate **13** could not be obtained this way. We next considered electrophilic fluorination of the methylene phosphonate **15**, a reaction similar to that reported by Robins for the fluorination of methylenephosphonatesulfonates.[9]

The synthesis of the diethyl phosphonate analogue of **15** has already been described,[4] and we used the same methods for the construction of the dimethyl phosphate **15**. Thus, treatment of bis-methyl ester **14** with $LiCH_2P(O)(OMe)_2$ gave **15** in modest yield. Treatment of **15** with NaH, followed by the addition of one equivalent of selectfluor [1-chloromethyl-4-fluoro-1,4-diazoniabicyclo[2.2.2]octane bis-(tetrafluoroborate)], however, led to the formation of the undesired difluorophosphonate **16** (40%) and recovery of starting material **15** (55%). This is presumably because the monofluorinated product is more acidic than the starting material and deprotonates and fluorinates a second time. Reverse addition (i.e. adding the preformed sodium salt of **15** to two equivalents of selectfluor) was more successful, giving a 50% yield of the desired **17**, 16% of the difluorophosphonate **16** and the remainder as starting material **15** (20%). These compounds were easily separated by using flash chromatography. The protected monofluorophosphonate **17** exists as a mixture of diastereomeric (roughly 45%:45%) and enol (10%) forms as shown by ^{19}F NMR. Thus, no attempt was made to separate the diastereomers. The mixture was deprotected by using the in situ generation of TMS-I (TMSCl and NaI in CH_3CN) followed by KOH hydrolysis of the resulting TMS esters. ^{19}F NMR of the product **7** showed the presence of approximately 1% of the enol isomer and equimolar amounts of each diastereomer.

The synthesis of the acetylenic phosphonate **10** has been described previously, but in racemic form.[10] An initially attempted Ohira–Bestmann reaction[11] of the doubly BOC-protected (BOC = *tert*-butyloxycarbonyl) enantiomerically pure aminoaldehyde **18**[4] gave the aldehyde **19**, but in low yield (Scheme 3). However, we realised that the methylene phosphonate **15** could be converted to the required alkyne if the ketone could be enolised and eliminated. Thus **15** was treated with triflic anhydride and DIPEA. Under these conditions the intermediate triflylenolether was not observed, and the protect-

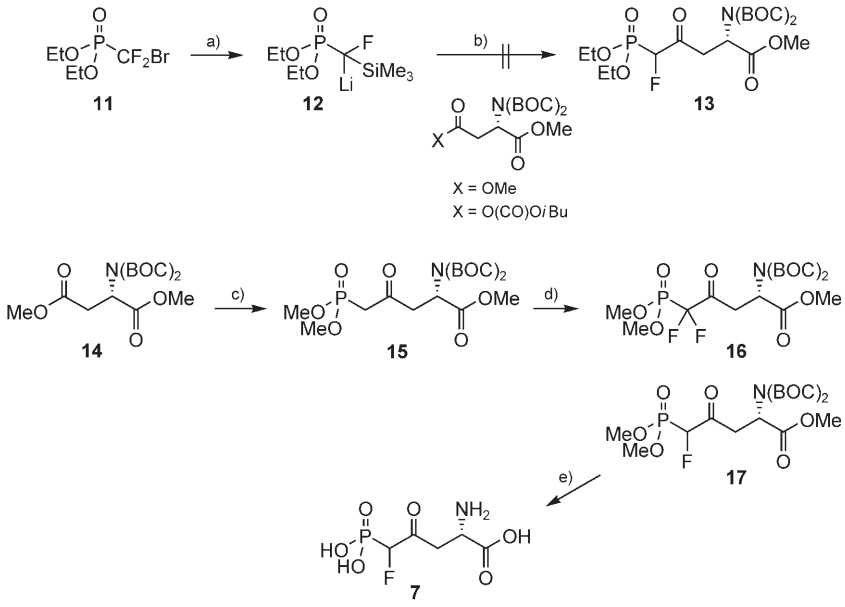

Scheme 2. Route to monofluromethylenephosphonate **7**. a) BuLi, Me_3SiCl, BuLi, −78 °C; b) addition of electrophile, −78 °C; c) $(MeO)_2P(O)CH_3$, BuLi, −78 °C to RT, 29%; d) NaH, THF, 0 °C, then selectfluor, −10 °C, 50%; e) CH_3CN, Me_3SiCl, NaI, RT, then KOH(aq), 70%.

ed L-alkyne **20** was obtained in moderate yield. Deprotection was achieved in refluxing aqueous HCL to give the L-amino acid **10** in quantitative yield.

Initial attempts to reduce the protected alkyne **20** focused on the use of zirconium reagents such as Schwartz reagent (Cp_2ZrHCl) and Negishi's reagent ($Cp_2ZrCl_2/2\,BuLi$). Attempts to add the Schwartz reagent to **20** followed by aqueous hydrolysis were unsuccessful, and Quntar and Srebnik's method involving the addition of Negishi's reagent to acetylenic phosphonates to form zirconacycles, which can be hydrolysed to *Z*-olefins, was also unsuccessful.[12] Removal of one of the BOC protecting groups of **20** gave the monoprotected amine **21**—however, this was similarly unreactive to the Zr reagents.

Traditional Lindlar conditions proved more useful for the controlled reduction of the mono-BOC acetylene **21**, giving a 75% yield of the desired *Z*-olefin **22** and 21% of the over-reduced analogue **23** (Scheme 4). The *Z*-selectivity is reflected in the coupling constants of the ^1H spectrum of **22**. Savignac showed that for the *E*-vinyl phosphonates typical coupling constants are $^3J_{HH\text{-}trans}$ values of 17.1–17.3 Hz and $^3J_{PH\text{-}cis}$ values of 20–23 Hz; for *Z*-vinyl phosphonates typical values are $^3J_{PH\text{-}trans}=38$–50 Hz and $^3J_{HH\text{-}cis}=5$–13 Hz.[13] The *Z*-vinyl phosphonate **22** displayed typical coupling values for such compounds; $^3J_{PH\text{-}trans}=52.4$ Hz and $^3J_{HH\text{-}cis}=13.2$ Hz. The *Z*-olefin and over-reduced compound were conveniently separated by flash chromatography and deprotected in refluxing aqueous HCl, giving **9** and **24**, respectively, in quantitative yields.

The synthesis of the *E*-olefin **8** also proved troublesome initially. We attempted the metathesis approach pioneered by Hayes[14] in which dimethylvinyl phosphonate **25** was treated with protected allylglycine **26** (Scheme 5) in the presence of the Grubbs second-generation catalyst, but this did not yield the desired olefin **27**, and only starting material was recovered. A more conventional approach, involving the Horner–Wadsworth—Emmons-type reaction of the doubly BOC-protected aldehyde **18**[4] with the bisphosphonate **31** was more successful, however, affording the desired protected olefin **28** in 80% yield. The *E* selectivity of the reaction is apparent from the coupling constants in the ^1H NMR spectrum.[13] The vinyl phosphonate **28** has coupling constants typical for a *trans*-alkene ($^3J_{HH}=17.1$ and $^3J_{PH}=21.5$ Hz). Confirmation of the structure was gained by crystal structure analysis of **28** (Figure 1). Deprotection to **8** was again achieved in quantitative yield by aqueous acid hydrolysis.

Modification of this reaction provided the fluorinated olefin **29**. Thus the bisphosphonate **31** was treated with base and then selectfluor to give the monofluorophosphonate **32** in 50% yield. A second deprotonation and treatment with the doubly BOC-protected amino aldehyde **18** gave a low yield of the monofluoro-olefin **29**. However, sufficient material was obtained for deprotection to **30** and further study.

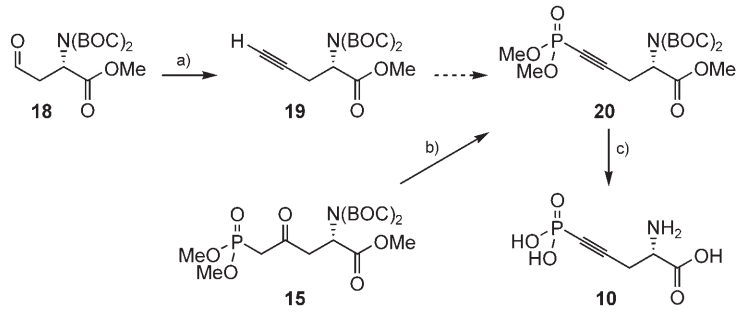

Scheme 3. Route to acetylenic analogue **10:** a) K_2CO_3, MeOH, 0 °C, then $(MeO)_2P(O)C(N_2)C(O)CH_3$, 12%; b) CH_2Cl_2, 0 °C, DIPEA, Tf_2O, 57%; c) HCl(aq), Δ, 99%. DIPEA = *N*,*N*-diisopropylethylamine.

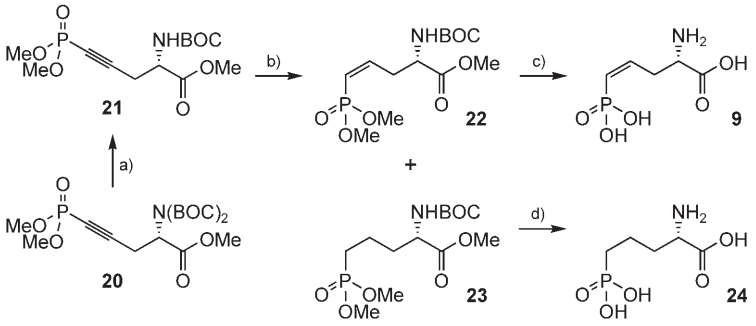

Scheme 4. Synthetic routes to *Z*-olefinic and saturated analogues**:** a) CH_2Cl_2, CF_3CO_2H, RT, 68%; b) MeOH, $Pd/BaSO_4$/quinoline, H_2 (1 atm), RT, 45 min, 75%; c) HCl(aq), Δ, quant.; d) HCl(aq), Δ, quant.

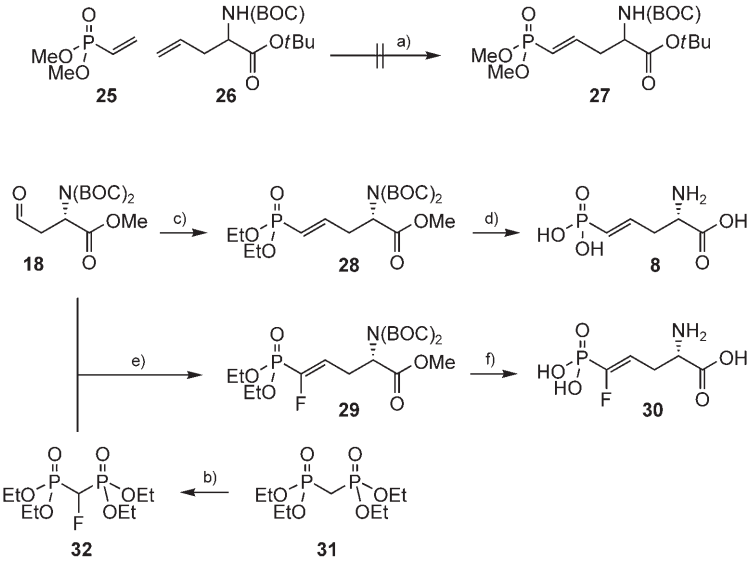

Scheme 5. Synthesis of *E*-olefinic analogues**:** a) $RuCl_2(^iMES)(PCy_2)CHPh$, CH_2Cl_2, RT; b) THF, NaH, selectfluor, 53%; c) **31**, NaH, THF, 0 °C, 65%; d) HCl(aq), Δ, 99%; e) NaH, THF, 0 °C, 8%; f) HCl(aq), Δ, 99%.

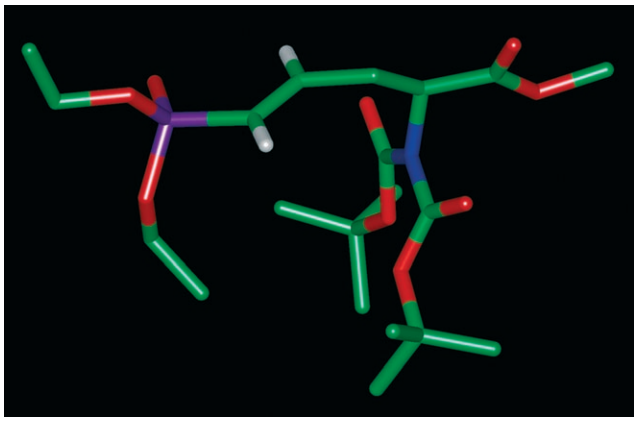

Figure 1. X-ray crystal structure of **28**, showing *E*-olefin. Aliphatic hydrogen atoms were removed for clarity.

Inhibition

ASA-DH is difficult to assay in the biosynthetic forward direction because of the instability of the substrate aspartylphosphate **1**. However, L-aspartate semialdehyde **3** is simply prepared by ozonolysis of L-allylglycine.[15] This is then used as the substrate for the enzyme, and turnover is monitored by detecting the production of NADPH from $NADP^+$ at 340 nm in the presence of high phosphate concentrations, from which the rate of reaction can easily be measured (Scheme 6).[4] Two types of assays were used: "competitive" assays to detect reversible inhibition were performed by adding the inhibitor to the standard assay; and time-dependent inhibition was detected by preincubating ASA-DH with the inhibitor, in the absence of substrates, and measuring the amount of uninhibited enzyme remaining at subsequent time points by using the standard assay procedure.

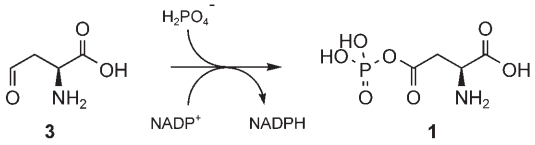

Scheme 6. Assay procedure for ASA-DH.

The monofluoromethylene phosphate **7** behaved similarly to the difluoromethylene phosphonate **4** previously studied.[4] In competitive assays, no inhibition was observed; however, when **7** was incubated with ASA-DH in the absence of phosphate and substrates, inhibition was observed that varied over time (Figure 2). In the case of **4** this inhibition is reversible,[4] as it was observed that when ASA-DH inhibited with **4** was added to assay mixtures containing phosphate, ASA and NADPH, the initial slow rate of reaction increased over time, thus indicating loss of inhibitor from the active site. In contrast, this behaviour was not observed for inhibition of ASA-DH by **7**. Instead, inhibited ASA-DH did not regain activity when diluted into solutions containing substrates (even after prolonged incubation), indicative of irreversible covalent inhibition. However, inhibition was weak with a measured K_i of 1.2 mM.

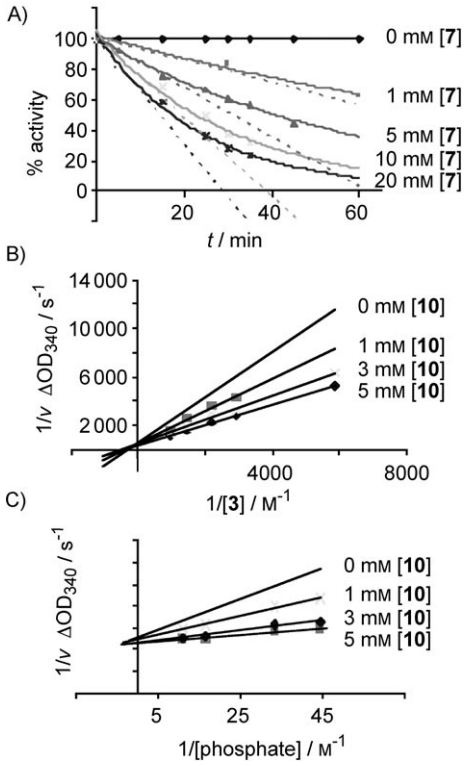

Figure 2. Inhibition of ASA-DH by **7** and **10**: A) residual activity plot for inhibition by **7**; B) Reciprocal rate data for inhibition of ASA-DH with varying ASA and **10** concentrations; C) Reciprocal rate data for inhibition of ASA-DH with varying phosphate and **10** concentrations.

The *E*-vinylphosphonate **8** also showed no observable reversible inhibition at concentrations up to 20 mM, and was inactive in time-dependent assays at this high concentration. The fluorinated vinylphosphonate **30** was also inactive in both assays. The *Z*-olefin **9** showed very marginal reversible inhibition at 20 mM and no time-dependent inhibition. However, the acetylene **10** showed relatively good reversible inhibition of ASA-DH; variation of **3**, phosphate and **10** concentrations showed that **10** is a competitive inhibitor versus both **3** and phosphate, with K_i values of 3.9 mM versus **3** and 1.3 mM versus phosphate (Figure 2). No time-dependent inhibition was observed for **10.** The fully reduced compound **24** was also tested as an inhibitor of ASA-DH, but showed no observable activity at concentrations up to 20 mM.

Discussion

Our previous results suggested that initial recognition and binding of substrates by ASA-DH is controlled, to a large extent, by the charge on the phosphate group—monoanionic compounds are preferred to dianions. This is consistent with a singly charged cationic arginine residue in the active site of ASA-DH (vide infra). This analysis is borne out by the behaviour of the monofluoromethylene phosphonate **7**. This compound would be expected to have a pK_{a_2} value of around 6.2, and so

the phosphonate of **7** would be largely di-ionised at pH 8.6 of the inhibition assay. Thus, this compound did not compete well with phosphate itself, but, as expected, **7** proved to be a time-dependent inhibitor of ASA-DH in the absence of phosphate.

The inhibitory activity of the other compounds is harder to understand based on pK_a arguments—the pK_{a_2} values for the olefins and acetylene would be expected to be around 8.0 and 6.5, respectively, but the acetylene showed significantly better competitive inhibition than either olefin. We reasoned that this is probably a reflection of geometric considerations. In order to assess this possibility, simulated docking procedures were used to model the interactions and likely geometries of the substrate **1** and inhibitors studied here.

X-ray crystal structures of ASA-DH from *E. coli* have been previously obtained.[1,16] In particular, one structure exists in which a substrate analogue is covalently attached to the active-site cysteine and in which a flexible loop region (Asp231–Glu242) has become more ordered over the top of the active site.[1,16] The substrate mimic was manually removed from the coordinate file (Protein Data Bank ID: 1gl3), and this was used for simulated docking experiments with the Sybyl software package (Tripos Software). The first simulated docking experiment performed was with the substrate **1**. In the resulting structure, substrate **1** takes up a conformation in which the phosphate interacts with Arg102 and the carboxylate interacts with Arg267 (Figure 3A). This is in agreement with crystal structure data obtained by Viola, in which ASA **3** is covalently bound as a thiohemiacetal in the active site of *H. influenzae* ASA-DH (corresponding to intermediate B in Scheme 1). In this structure the carboxylate of the covalently bound ASA **3** interacts with an arginine corresponding to Arg267 of the *E. coli* enzyme and a free phosphate ion interacts with an arginine which corresponds to Arg102 of the *E. coli* enzyme.[17]

The carbonyl carbon atom of the docked substrate **1** lies 4.4 Å from the cysteine thiol group in the docked structure. Although this distance does not represent a bonding interaction (the bond length is 1.8 Å in the ASA-thiohemiacetal structure of Viola), it is clear from the fact that bonding does occur, that electrophilic carbon atoms that can locate 4.4 Å or less from the thiol have the potential to bind covalently, given the correct geometrical constraints. The carbonyl group of docked **1** also points at the active-site His274; this might play a role in polarising the carbonyl prior to nucleophilic attack and deprotonating the thiol nucleophile. Thus the simulated docking procedure we used appears to predict the likely bound conformation of the substrate (prior to covalent bond formation) well.

We next used the same procedure to model the docking of the known inhibitors **4** and **5**. Both compounds took up very similar docked conformations to the substrate **1**—the phosphate interacts with Arg267, while the carboxylate interacts with Arg102. For the difluoromethylene phosphonate **4**, the nucleophilic carbonyl is 4.3 Å from the nucleophilic cysteine thiol, while for the methylene phosphonate it is 3.9 Å away—both within the distance obtained for **1**. Again, the carbonyls of **4** and **5** point towards the active-site histidine.

The acetylene **10** behaved similarly: the phosphate and carboxylate locate correctly, but the electrophilic carbon of the alkyne is far from the cysteine sulfur atom (6.4 Å), and, in any case, the two are poorly aligned for reaction (Figure 3B). The simulated docking of the two olefins **8** and **9** was examined next. The *Z*-olefin **9** also appeared to dock successfully—both carboxylate and phosphate can interact with the two arginines (Figure 3C). In this structure, the active-site thiol is close to the electrophilic carbon atom (3.8 Å), but is not orientated correctly for nucleophilic attack. The *E*-olefin **8** did not take up a conformation likely to lead to effective binding—the rigidity of the compound prevented it reaching a conformation in which both the phosphate and carboxylate could interact with the two active-site arginines (Figure 3D). In the structure shown in Figure 3D, the distance between the active-site thiol and the electrophilic alkene carbon atom is 4.8 Å.

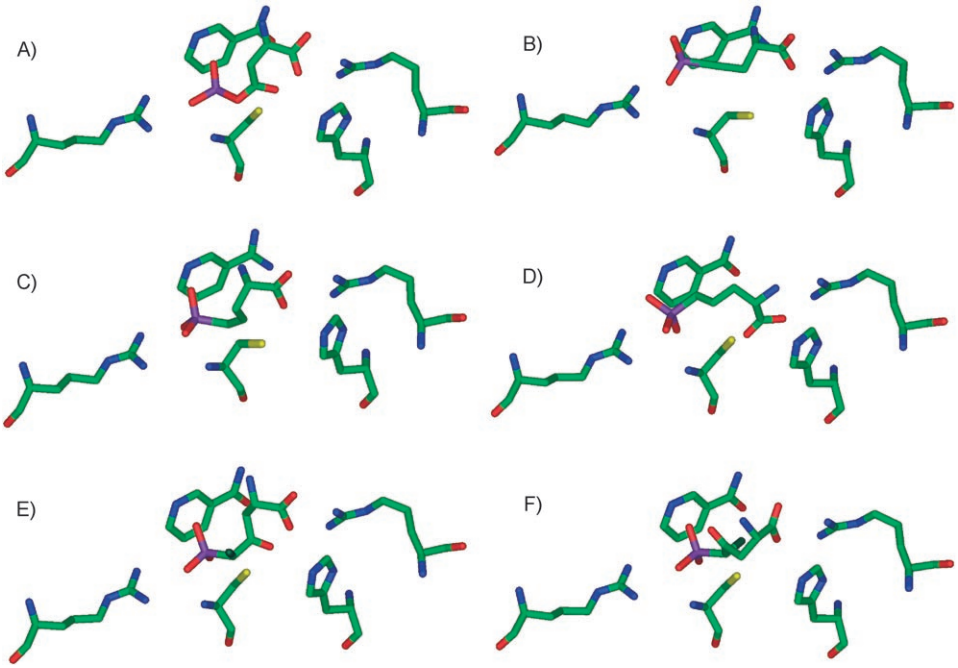

Figure 3. Substrates and inhibitors of ASA-DH interacting with active-site residues of ASA-DH obtained by simulated docking. In each case the four active-site residues are (from l to r) Arg102, Cys135, His274, and Arg267, with the nicotinamide moiety of $NADP^+$ shown behind: A) substrate **1**; B) alkyne **10**; C) *cis*-olefin **9**; D) *trans*-olefin **8**; E) 5*R*-fluoride **7a**; F) 5*S*-fluoride **7b**.

Both diastereomers of the monofluorophosphonate **7** were then modelled into the active site of ASA-DH. The (2*S*,5*R*) isomer **7a** takes up a conformation very similar to that observed for the other compounds, with a carbonyl–thiol distance of 4.0 Å (Figure 3E). However, the (2*S*,5*S*) isomer **7b** takes up a conformation different to that observed for the other compounds—while the carboxylate and phosphate still interact with Arg102 and Arg267, respectively, the carbonyl group has rotated so that it is no longer interacting with the active-site histidine residue and has moved to be 6.0 Å away from the active-site thiol (Figure 3F). The model also suggests a plausible explanation for the irreversible inhibition by **7**. Thiohemiacetal formation between the active-site thiol of ASA-DH and the carbonyl of **7** would be expected to be reversible, unlike the observed irreversible inhibition. However, displacement of fluoride from the phosphonate carbon atom by the active-site thiol would be expected to lead irreversibly to a covalent adduct. In the case of docked **7a**, the phosphonate CHF carbon atom lies 4.32 Å away from the thiol, while for **7b** this distance is 4.05 Å. However, in the predicted structure of docked **7a**, the active-site thiol approaches at a near perfect angle for S_N2 attack (176.7°), while for **7b** the angle is 64.9°, an angle unlikely to lead to covalent bond formation.

The modelling studies clearly reflect the trends observed in the inhibition data. For example, the *E*-olefin **8** did not dock well into the active site of ASA-DH and did not show any inhibitory activity. The *Z*-olefin **9** and acetylene **10** docked better and showed better competitive inhibition. Neither of these compounds showed time-dependent inhibition as their electrophilic carbonyls were located too far away from the thiol and, in any case, were incorrectly aligned for bond formation.

The only compound to show measurable time-dependent inhibition was the monofluorophosphonate **7**. Here, one isomer of **7**, the (2*S*,5*R*) isomer **7a**, takes up a conformation in which both the phosphate and carboxylate can make productive interactions with the active-site arginines. In this structure the thiol is located 4.3 Å away from the phosphonate CF at a near perfect angle for S_N2 attack; this could lead to the observed irreversible inhibition. Inhibition is weak because initial binding is controlled by the phosphate pK_{a_2} such that a doubly ionised phosphate is poorly recognised.

To date, inhibitors based on the structure of the substrate **1** have shown modest inhibition—with K_i values in the region of the reported K_M values for substrates.[4] This is unsurprising as most structural features of the substrate are retained in the inhibitors and the substrates themselves do not bind tightly to the enzyme. For the design of more potent future inhibitors of ASA-DH, compounds that could be useful antimicrobial agents, more drastic structural changes will have to be considered. However, we have shown that simulated docking approaches may be useful in the design of such compounds.

Experimental Section

Procedures for the synthesis of compounds **7**–**10**, **15**–**17**, **19**–**24**, **28**–**30**, and **32**, as well as assay procedures are contained in the Supporting Information.

Acknowledgements

J.S.G. thanks the School of Chemistry, University of Bristol, for studentship funding.

Keywords: enzymes · inhibitors · phosphonates · simulated docking · synthesis design

[1] A. Hadfield, C. Shammas, G. Kryger, D. Ringe, G. A. Petsko, J. Ouyang, R. E. Viola, *Biochemistry* **2001**, *40*, 14475.
[2] J. Blanco, R. A. Moore, C. R. Faehnle, R. E. Viola, *Acta Crystallogr. Sect. A* **2004**, *60*, 1808.
[3] O. S. Harb, Y. Abu Kwaik, *Infect. Immun.* **1998**, *66*, 1898.
[4] R. J. Cox, J. S. Gibson, M. B. Mayo-Martin, *ChemBioChem* **2002**, *3*, 874.
[5] D. B. Berkowitz, M. Bose, T. J. Pfannensteil, T. Doukov, *J. Org. Chem.* **2000**, *65*, 4498.
[6] D. J. Martin, C. E. Griffin, *J. Organomet. Chem.* **1964**, *1*, 292.
[7] J. Neischalk, A. S. Batsanov, D. O'Hagan, J. A. K. Howard, *Tetrahedron* **1996**, *52*, 165.
[8] R. Waschbusch, J. Carran, P. Savignac, *Tetrahedron* **1997**, *53*, 6391.
[9] S. F. Wnuk, M. J. Robins, *J. Am. Chem. Soc.* **1996**, *118*, 2519.
[10] C. Harde, K. H. Neff, E. Nordhoff, K. P. Gerbling, B. Laber, H. D. Pohlenz, *Bioorg. Med. Chem. Lett.* **1994**, *4*, 273.
[11] P. Callant, L. Dhaenens, M. Vandewalle, *Synth. Commun.* **1984**, *14*, 155.
[12] A. A. Quntar, M. Srebnik, *Org. Lett.* **2001**, *3*, 1379.
[13] M. P. Teulade, P. Savignac, E. E. Aboujaoude, S. Lietge, N. Collignon, *J. Organomet. Chem.* **1986**, *304*, 283.
[14] M. Lera, C. J. Hayes, *Org. Lett.* **2001**, *3*, 2765.
[15] S. Black, N. G. Wright, *J. Biol. Chem.* **1955**, *213*, 39.
[16] C. E. Nichols, B. Dhaliwal, M. Lockyer, A. R. Hawkins, D. K. Stammers, *J. Mol. Biol.* **2004**, *341*, 797.
[17] J. Blanco, R. A. Moore, R. E. Viola, *Proc. Natl. Acad. Sci. USA* **2003**, *100*, 12613.

Received: April 21, 2005
Revised: August 3, 2005
Published online on October 31, 2005

